Front. Phys. 13(4), 138101 (2018)
https://doi.org/10.1007/s11467-018-0747-5

RESEARCH ARTICLE

Vertically aligned γ-AlOOH nanosheets on Al foils as flexible and reusable substrates for NH_3 adsorption

Chen Yang[1], Ying Chen[1,†], Dan Liu[1], Jinfeng Wang[1], Cheng Chen[1], Jiemin Wang[1], Ye Fan[1], Shaoming Huang[2], Weiwei Lei[1,‡]

[1] *Institute for Frontier Materials, Deakin University, Locked Bag 2000, Geelong, Victoria 3220, Australia*
[2] *Nanomaterials & Chemistry Key Laboratory, Wenzhou University, Wenzhou 325035, China*
Corresponding author. E-mails: †ian.chen@deakin.edu.au, ‡weiwei.lei@deakin.edu.au
Received December 11, 2017; accepted January 9, 2018

Vertically aligned γ-AlOOH nanosheets (NSs) have been successfully fabricated on flexible Al foils via a solvothermal route without morphology-directing agents. Three different reaction temperature (25, 80, and 120 °C) and time (30 min, 45 min, and 24 h) are discussed for the growth period, which efficiently tune the density and size of the γ-AlOOH NSs. Meanwhile, the growth speed of the nanosheets confirms that dominant growth stage is seen in the initial 45 min. Furthermore, the interlayer of the γ-AlOOH NSs displays an average height of 140 nm and superhydrophilicity. By dynamic adsorption, the as-synthesized γ-AlOOH NSs exhibit an outstanding NH_3 adsorption capacity of up to 146 mg/g and stably excellent regeneration for 5 cycles. The mechanism of NH_3 adsorption on the in-plane of the γ-AlOOH NSs is explained by the Lewis acid/base theory. The H-bond interactions among the NH_3 molecules and the edge groups (-OH) further improve the capture ability of the nanosheets.

Keywords γ-AlOOH nanosheets, NH_3 adsorption, Lewis acid/base theory, H bonds interaction

1 Introduction

Ammonia (NH_3) as an alkaline and toxic gas, which is mainly from NH_3-contained fertilizers and waste treatment industries including the manufacturing of nitric acid, refrigeration systems and sewage treatment plants, has caused air pollutions and threatened human being's health [1, 2]. Significant efforts have been devoted presently into the exploration and creation of sorbents materials for gas and pollutants capture, such as multiple-wall carbon nanotubes [3, 4], graphite oxides [5], metal organic framework [6, 7], zeolite [8], metal oxides [9], porous BN nanosheets [10, 11] and their corresponding composites [12–16]. However, these materials usually exhibit a low adsorption capacity and poor recyclability. Therefore, the construction of novel gas adsorption nanomaterials with flexible substrates not only addresses practical usage requirement such as the special size, shape or position, but also can be fabricated and designed into specific gas capture devices.

Recently, γ-AlOOH (boehmite) materials with 3D flower-like nanostructures [17–20] or hollow spheres architectures [21–23] have been investigated extensively for scientific and industrial applications including supporting materials [24, 25], water purification [20, 26–28], Al_2O_3 ceramics transformation [29–31], optical materials [32] and composite materials [27, 28, 33] due to their fascinating properties of high elastic modulus, thermal and chemical stability, and good optical characteristics [32]. The conventional solution-based synthesis methods, for instance, solvothermal and hydrothermal routes [17, 20, 21, 24, 34–40], have been developed as the mainstream strategies for the preparation of 2D γ-AlOOH NSs. However, the methods always need the post-purification operation due to the addition of Al-based salts as the Al sources and organic chemicals as the morphology-directed agents.

Up to now, several reports have provided more environmental friendly and facile approaches to synthesize γ-AlOOH NSs using metal Al and water to replace Al-based salts and organic agents to control the nanostructures. For example, γ-AlOOH NSs were prepared on thick Al plates in the boiling water condition to in-

*Special Topic: Graphene and other Two-Dimensional Materials (Eds. Daria Andreeva, Wencai Ren, Guangcun Shan & Kostya Novoselov).

vestigate the properties of mechanically durable superrepellent surface [41]. Similarly, a thin Al layer was firstly deposited on the glass substrates for the preparation of vertically leaf-like γ-AlOOH NSs by hydrothermal synthesis. And then, large Au nanoparticles decorated on the top of γ-AlOOH NSs as 3D substrates for surface-enhanced Raman scattering study [42]. To the best of our knowledge, γ-AlOOH nanoflakes have been applied for gaseous HCHO adsorption [43], however, no research works of γ-AlOOH NSs are reported for the alkaline NH_3 gas capture.

Here, we report on the unprecedented development of perpendicular γ-AlOOH NSs on Al foils (denoted as γ-AlOOH NSs/Al) as flexible substrates for gas adsorption by the solvothermal method. The γ-AlOOH NSs/Al exhibits a good NH_3 adsorption ability around 146 mg/g with an excellent reusable capture performance for 5 cycles. Furthermore, the contact angle test confirms that the surface of γ-AlOOH NSs/Al displays a fascinating super-hydrophilicity of 7.9°. Therefore, this work provides a facile and high effective approach to configure vertically well-aligned γ-AlOOH NSs on Al foils for air purification and treatment.

2 Experimental

2.1 Specimen preparation

In a typical procedure, Al foils (thickness about 15 μm) were firstly cut into the circular shape with a diameter about 1.5 cm and washed by water and ethanol several times to remove the organic contaminations on the surface. Secondly, vertically aligned γ-AlOOH NSs grew on two sides of the Al foil in mixed solution system (20 mL DMF and 5 mL H_2O) at 120°C for 1 h. Finally, as-resulted samples were cleaned by ethanol solution several times to remove DMF contaminations and dried in air.

2.2 NH_3 adsorption test

50 pieces of γ-AlOOH NSs/Al were put into to the test chamber and sealed. The certain concentration of selected NH_3 odour around 0.15–0.16 mg/L was injected into the pump. The odour quickly went through the pump and the testing chamber with the volume of 8 L, and then circulated in the sealed gas detection system. The signal of N-H bond from NH_3 gas was detected by Infra-red spectrometer and reflected the change of the NH_3 concentration. All adsorption equilibrium data were collected for 48 h at room temperature and the adsorption pressure was 1 atm. The NH_3-saturated γ-AlOOH NSs/Al were outgassed in the vacuum oven at 80°C for 5 h to regenerate capture ability.

2.3 Calculation of NH_3 adsorption ability

Aiming to acquire and reflect the strong removal performance, the equation was adopted as

$$C = \frac{8L \times (C_e - C_0)}{50 \times \rho \times 2 \times \pi r^2 h}, \quad (1)$$

where C represented the adsorption capacity of NH_3, while C_e and C_0 meant the concentration of NH_3 at initial and equilibrium stage, respectively. The ρ, r, and h were the density of γ-AlOOH, diameter of Al foil and height of vertical γ-AlOOH, respectively.

2.4 Characterization

The unique surface nanostructures were carried out by SEM (Zeiss Supra 55 VP) and TEM (JEOL 2100 LaB6 instrument, 200 kV). The chemical constituents were characterized by Raman (Renishaw confocal micro-Raman spectrometers, 633 nm lasers) and FTIR spectroscopy (recorded by attenuated total refraction method, Bruker Vertex 70 equipped with a Pike Miracle diamond crystal). The contact angle test of the γ-AlOOH NSs/Al surface was corroborated by Attension Theta instrument. NH_3 adsorption was run using Miran 1A Infra-red spectrometer.

2.5 Results and discussion

The top-view scanning electron microscopy (SEM) image [Fig. 1(a)] illustrated that γ-AlOOH NSs densely grew in a well-ordered fashion on Al foils with an average length of 100–300 nm. Essentially, Al foils directly acted as Al sources and support substrates during the solvothermal process. The vertical morphology and average thickness around 140 nm were confirmed by the side-view SEM image [Fig. 1(b)]. Meanwhile, transmission electron microscopy images (TEM) exhibited a high-crystallized nanosheets structure. Moreover, the inter-spacing between adjacent fringes was around 0.241 nm assigned to the (031) lattice plane of γ-AlOOH NSs as shown in the inserted image [Fig. 1(c)] [24]. The judgement of the crystalline structure and classification of chemical bonds of γ-AlOOH NSs were identified by the characteristic peaks from Raman and FT-IR spectroscopy, respectively. The obvious Raman shift observed at 362 cm^{-1} was attributed to the symmetric mode of Al-O vibration (Fig. A1 in the Appendix) [44]. The typical FT-IR image [Fig. 1(d)] demonstrated that the strong and broad bands at 3309 and 3093 cm^{-1} discharged from the stretching vibration of -OH group of the adsorbed water and symmetric stretching vibration of AlO-H, respectively [18, 39]. Furthermore, the peak located at 1652 cm^{-1} was considered as the feature of the bending mode of the absorbed water [31, 34, 45]. The intense

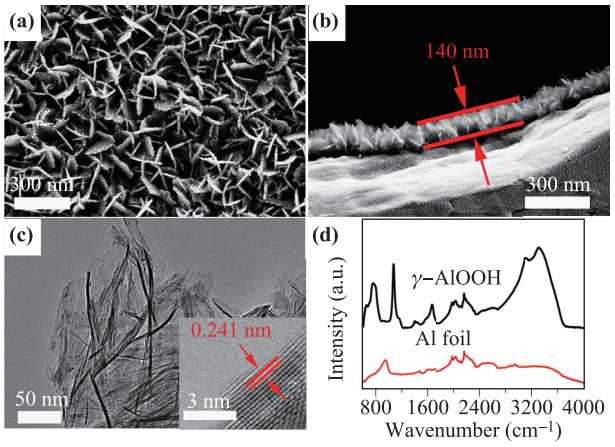

Fig. 1 **(a)** Top- and **(b)** side-view of SEM images; **(c)** TEM and HRTEM inserted images; **(d)** FT-IR spectroscopy of γ-AlOOH NSs and pure Al foil.

band at 1072 cm^{-1} belonged to the bending vibration mode of Al-O-H and bands at 752 and 648 cm^{-1} were consistence with the vibration mode of AlO_6 [18, 39, 46].

To further understand the role of reaction temperature during the synthesis and self-assembly process, three different temperatures (25, 80, and 120°C) were chosen to produce γ-AlOOH NSs under 24 h. SEM images demonstrated that in contrast with 120°C, the room temperature of 25°C was not beneficial to facilitate the growth of γ-AlOOH NSs and relatively sparse γ-AlOOH NSs could be obtained at 80°C [Figs. 2(a), (c), and (e)]. In addition, the reaction time could tune the fabrication of γ-AlOOH NSs as another important factor. Three different time (30 min, 45 min, and 24 h) were used to synthesize γ-AlOOH NSs under 120°C, respectively. Combining with the statistic of the length, SEM images further indicated that small and sparse γ-AlOOH NSs with an average length of 56 nm were acquired at initial 30 min [Fig. 2(b) and Fig. A2(a) in the Appendix]. Once the time prolonged to 45 min and even 24 h, the density of γ-AlOOH NSs reached up to the similar optimal states as well as the length around 150 nm and 155 nm, respectively [Figs. 2(d) and (f); Figs. A2(b) and (c) in the Appendix]. Consequently, γ-AlOOH NSs were prepared and assembled perpendicularly on Al foils before 30 min with the growth speed of 1.87 nm/min, while the density and size increased fast during the following 15 min with the growth speed up to 6.27 nm/min. From 45 min to 24 h, γ-AlOOH NSs preferred to stop the growth due to the super-low growth speed of 0.0036 nm/min, as shown in Fig. A2(d) in the Appendix. Hence, the synthesis and self-assembly process was also a time-controlled process and optimized synthesis time was at least 45 min.

To evaluate the performance of NH_3 capture, γ-AlOOH NSs were tested by the dynamic adsorption method. Figure 3(a) displayed the rapid adsorption performance before 5 h, implying that γ-AlOOH NSs possessed a huge potential for NH_3 removal. Using Eq. (1), it was surprisingly found that γ-AlOOH NSs exhibited an excellent NH_3 adsorption ability with a high capacity up to 146 mg/g at the initial cycle. Furthermore, the good adsorption ability of γ-AlOOH NSs could be highly effective recovered by simple heating treatment in a conventional oven. Therefore, the cycling tests were carried out and γ-AlOOH NSs remained a stable adsorption performance around 143 mg/g at the 5^{th} cycle, as shown in Fig. 3(b). The excellent adsorption behaviours could be explained by the Lewis acid/base interaction and hydrogen bonding. The vertical γ-AlOOH NSs provided a large contact surface and exposed extensively O atoms with lone pair electrons as nucleophilic species. On the base of the Lewis acid/base interaction theory, the electrophilic behaviour existed between H atoms in NH_3 molecules and O atoms on the in-plane surface of the γ-AlOOH NSs, indicated by the black rectangular box as shown in Fig. 3(c). Moreover, the formation of weak H bonds from NH_3 and edged -OH groups also promoted the adsorption performance presented by the yellow dotted line in Fig. 3(c). Additionally, the hydrophobicity of pure Al foil was 87.8°. However, the γ-AlOOH NSs interface displayed the super-hydrophilicity about 7.9° (Fig. A3 in the Appendix). It implied that the interface of γ-AlOOH NSs might capture the moisture from

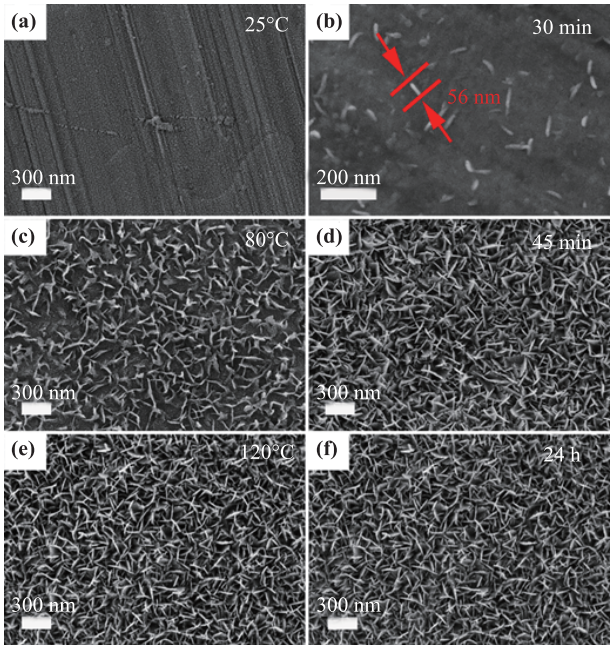

Fig. 2 SEM images of γ-AlOOH NSs on the Al foil at different temperatures of 25°C **(a)**, 80°C **(c)**, and 120°C **(e)** for 24 h; at various time of 30 min **(b)**, 45 min **(d)**, and 24 h **(f)** for 120°C.

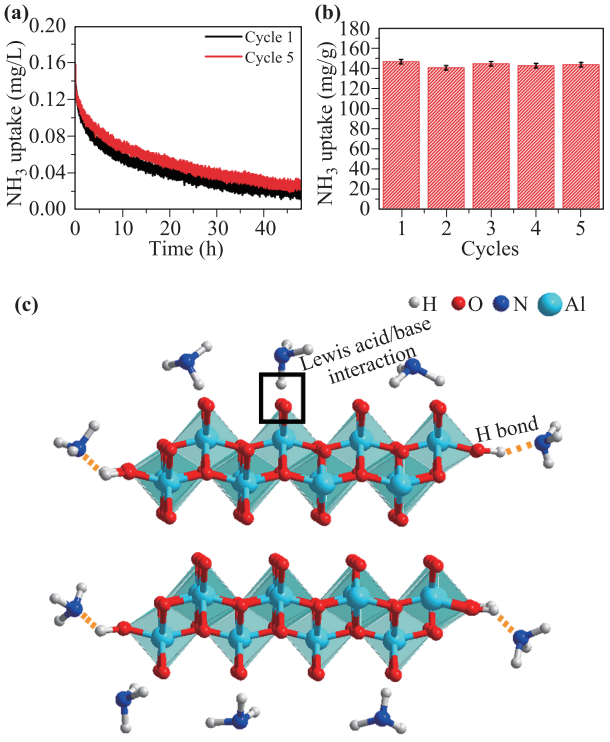

Fig. 3 **(a)** NH_3 adsorption at first and fifth times; **(b)** cycling tests for 5 times of NH_3 captures; **(c)** adsorption sites of γ-AlOOH NSs with NH_3 molecules.

air to dissolve NH_3 molecules, leading to the further increased adsorption behaviours.

3 Conclusions

In summary, we have successfully developed vertically aligned γ-AlOOH NSs on flexible Al foils by a one-step facile solvethermal route. The reaction temperature and time realize the controlled density and affect the growth speed of γ-AlOOH NSs, respectively. Moreover, the γ-AlOOH NSs exhibited the outstanding NH_3 capture ability up to 146 mg/g and reusable performance for 5 cycles. Combined with the numerous -OH groups, polar surface and specific nanostructures, γ-AlOOH NSs possess several advantages for the gas adsorption including enriched capture sites, high adsorption capacity and rapid recovery ability. Therefore, it proposes a facile and practical approach to produce flexible substrates for NH_3 capture, indicating the huge potential in commercial applications of gas adsorption.

Acknowledgements This work was financially supported by the Australian Research Council Discovery Program, the Australian Research Council Discovery Early Career Research Award scheme (DE150101617 and DE140100716), and Central Research Grant Scheme of Deakin University.

Appendix A Supporting information

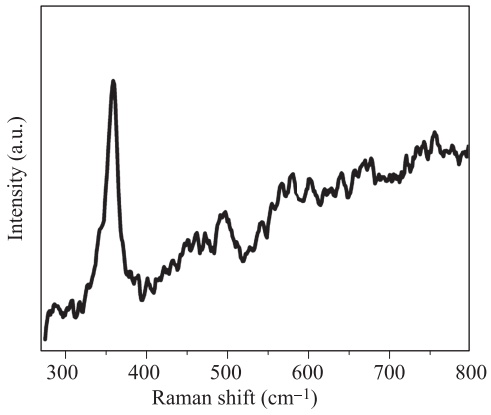

Fig. A1 Raman spectroscopy of the resultant vertical γ-AlOOH NSs on Al foils.

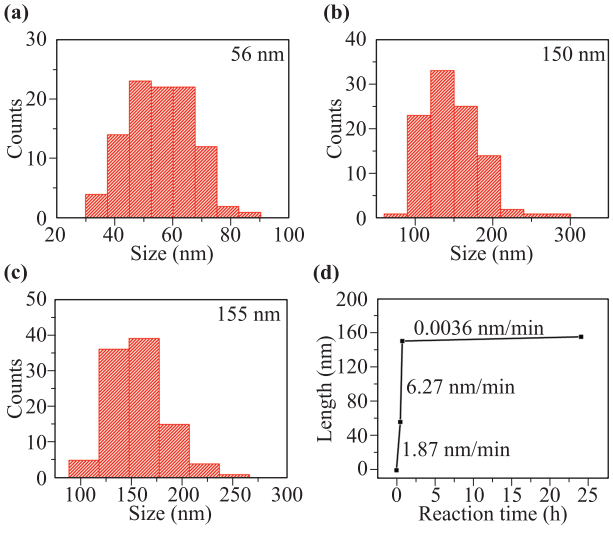

Fig. A2 Statistic of the length of γ-AlOOH NSs at **(a)** 30 min, **(b)** 45 min, and **(c)** 24 h; **(d)** the change of the length and growth speed of γ-AlOOH NSs.

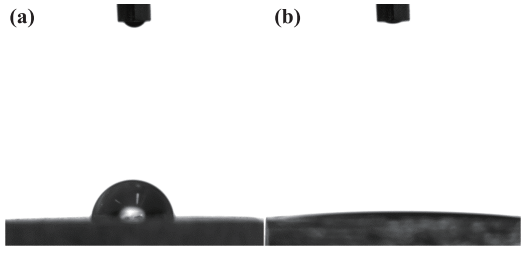

Fig. A3 Contact angle test: **(a)** pure Al foil and **(b)** γ-AlOOH NSs/Al.

References

1. A. Qajar, M. Peer, M. R. Andalibi, R. Rajagopalan, and H. C. Foley, Enhanced ammonia adsorption on functionalized nanoporous carbons, *Microporous Mesoporous Mater.* 218, 15 (2015)
2. J. B. DeCoste, M. S. Jr Denny, G. W. Peterson, J. J. Mahle, and S. M. Cohen, Enhanced aging properties of HKUST-1 in hydrophobic mixed-matrix membranes for ammonia adsorption, *Chem. Sci.* 7(4), 2711 (2016)
3. T. Yan, T. X. Li, R. Z. Wang, and R. Jia, Experimental investigation on the ammonia adsorption and heat transfer characteristics of the packed multi-walled carbon nanotubes, *Appl. Therm. Eng.* 77, 20 (2015)
4. T. Yan, T. X. Li, H. Li, and R. Z. Wang, Experimental study of the ammonia adsorption characteristics on the composite sorbent of $CaCl_2$ and multi-walled carbon nanotubes, *Int. J. Refrig.* 46, 165 (2014)
5. M. Seredych, J. A. Rossin, and T. J. Bandosz, Changes in graphite oxide texture and chemistry upon oxidation and reduction and their effect on adsorption of ammonia, *Carbon* 49(13), 4392 (2011)
6. Y. Chen, C. Y. Yang, X. Q. Wang, J. F. Yang, K. Ouyang, and J. P. Li, Kinetically controlled ammonia vapor diffusion synthesis of a Zn(II) MOF and its H_2O/NH_3 adsorption properties, *J. Mater. Chem. A* 4(26), 10345 (2016)
7. D. P. Saha and S. G. Deng, Ammonia adsorption and its effects on framework stability of MOF-5 and MOF-177, *J. Colloid Interface Sci.* 348(2), 615 (2010)
8. A. A. Halim, H. A. Aziz, M. A. M. Johari, and K. S. Ariffin, Comparison study of ammonia and COD adsorption on zeolite, activated carbon and composite materials in landfill leachate treatment, *Desalination* 262(1–3), 31 (2010)
9. D. Saha and S. G. Deng, Characteristics of ammonia adsorption on activated alumina, *J. Chem. Eng. Data* 55(12), 5587 (2010)
10. D. Liu, W. W. Lei, S. Qin, K. D. Klika, and Y. Chen, Superior adsorption of pharmaceutical molecules by highly porous BN nanosheets, *Phys. Chem. Chem. Phys.* 18(1), 84 (2016)
11. W. W. Lei, H. Zhang, Y. Wu, B. Zhang, D. Liu, S. Qin, Z. W. Liu, L. M. Liu, Y. M. Ma, and Y. Chen, Oxygen-doped boron nitride nanosheets with excellent performance in hydrogen storage, *Nano Energy* 6, 219 (2014)
12. C. Petit, L. L. Huang, J. Jagiello, J. Kenvin, K. E. Gubbins, and T. J. Bandosz, Toward understanding reactive adsorption of ammonia on Cu-MOF/graphite oxide nanocomposites, *Langmuir* 27(21), 13043 (2011)
13. C. Petit and T. J. Bandosz, Enhanced adsorption of ammonia on metal-organic framework/graphite oxide composites: Analysis of surface interactions, *Adv. Funct. Mater.* 20(1), 111 (2010)
14. C. Petit and T. J. Bandosz, Synthesis, characterization, and ammonia adsorption properties of mesoporous metal-organic framework (MIL(Fe))-graphite oxide composites: Exploring the limits of materials fabrication, *Adv. Funct. Mater.* 21(11), 2108 (2011)
15. S. Kang, J. Chun, N. Park, S. M. Lee, H. J. Kim, and S. U. Son, Hydrophobic zeolites coated with microporous organic polymers: adsorption behavior of ammonia under humid conditions, *Chem. Commun.* 51(59), 11814 (2015)
16. Y. Corre, M. Seredych, and T. J. Bandosz, Analysis of the chemical and physical factors affecting reactive adsorption of ammonia on graphene/nanoporous carbon composites, *Carbon* 55, 176 (2013)
17. G. C. Li, Y. Q. Liu, D. Liu, L. H. Liu, and C. G. Liu, Synthesis of flower-like Boehmite (AlOOH) via a simple solvothermal process without surfactant, *Mater. Res. Bull.* 45(10), 1487 (2010)
18. Z. B. Shi, W. Q. Jiao, L. Chen, P. Wu, Y. M. Wang, and M. Y. He, Clean synthesis of hierarchically structured boehmite and g-alumina with a flower-like morphology, *Microporous Mesoporous Mater.* 224, 253 (2016)
19. O. V. Bakina, E. A. Glazkova, N. V. Svarovskaya, A. S. Lozhkomoev, E. G. Khorobraya, and S. G. Psakhie, International Conference on Physical Mesomechanics of Multilevel Systems 2014, 1623, 35 (2014)
20. J. C. Xiao, H. H. Ji, Z. Q. Shen, W. Y. Yang, C. Y. Guo, S. J. Wang, X. W. Zhang, R. Fu, and F. X. Ling, Self-assembly of flower-like g-AlOOH and g-Al_2O_3 with hierarchical nanoarchitectures and enhanced adsorption performance towards methyl orange, *RSC Adv.* 4(66), 35077 (2014)
21. A. S. Lozhkomoev, E. A. Glazkova, N. V. Svarovskaya, O. V. Bakina, S. O. Kazantsev, and M. I. Lerner, International Conference on Advanced Materials with Hierarchical Structure for New Technologies and Reliable Structures 2015, 1683 (2015)
22. A. S. Lozhkomoev, E. A. Glazkova, O. V. Bakina, M. I. Lerner, I. Gotman, E. Y. Gutmanas, S. O. Kazantsev, and S. G. Psakhie, Synthesis of core–shell AlOOH hollow nanospheres by reacting Al nanoparticles with water, *Nanotechnology* 27(20), 205603 (2016)
23. Y. Y. Dong, Y. J. Liu, L. Y. Meng, B. Wang, M. G. Ma, and Y. Y. Li, Facile hydrothermal synthesis of Ag@AgCl@AlOOH hollow microspheres and their characterizations, *Mater. Lett.* 181, 204 (2016)
24. S. L. Liu, C. Y. Chen, Q. P. Liu, Y. W. Zhuo, D. Yuan, Z. H. Dai, and J. C. Bao, Two-dimensional porous g-AlOOH and g-Al_2O_3 nanosheets: Hydrothermal synthesis, formation mechanism and catalytic performance, *RSC Adv.* 5(88), 71728 (2015)
25. L. Zhang, and Y. J. Zhu, Microwave-assisted Solvothermal Synthesis of AlOOH hierarchically nanostructured microspheres and their transformation to g-Al_2O_3 with similar morphologies, *J. Phys. Chem. C* 112(43), 16764 (2008)

26. R. H. Sun, H. B. Zhang, J. Qu, H. Yao, J. Yao, and Z. Z. Yu, Supercritical carbon dioxide fluid assisted synthesis of hierarchical AlOOH@reduced graphene oxide hybrids for efficient removal of fluoride ions, *Chem. Eng. J.* 292, 174 (2016)
27. R. Kumar, M. Ehsan, and M. A. Barakat, Synthesis and characterization of carbon/AlOOH composite for adsorption of chromium(VI) from synthetic wastewater, *J. Ind. Eng. Chem.* 20(6), 4202 (2014)
28. R. Kumar, J. Rashid, and M. A. Barakat, Synthesis and characterization of a starch–AlOOH–FeS_2 nanocomposite for the adsorption of congo red dye from aqueous solution, *RSC Adv.* 4(72), 38334 (2014)
29. J. R. Wen, M. H. Liu, and C. Y. Mou, Synthesis of curtain-like crumpled boehmite and g-alumina nanosheets, *CrystEngComm* 17(9), 1959 (2015)
30. Z. Tang, J. L. Liang, X. H. Li, J. F. Li, H. L. Guo, Y. Q. Liu, and C. G. Liu, Synthesis of flower-like Boehmite (g-AlOOH) via a one-step ionic liquid-assisted hydrothermal route, *J. Solid State Chem.* 202, 305 (2013)
31. G. J. Ji, M. M. Li, G. H. Li, G. M. Gao, H. F. Zou, S. C. Gan, and X. C. Xu, Hydrothermal synthesis of hierarchical micron flower-like g-AlOOH and g-Al_2O_3 superstructures from oil shale ash, *Powder Technol.* 215-216, 54 (2012)
32. X. Y. Chen, H. S. Huh, and S. W. Lee, Hydrothermal synthesis of boehmite (γ-AlOOH) nanoplatelets and nanowires: pH-controlled morphologies, Nanotechnology 18, 285608 (2007)
33. K. H. Hu, Y. K. Cai, G. Q. Shao, and X. L. Cui, Synthesis and photocatalytic properties of nano-MoS_2/AlOOH composite, *React. Kinet. Mech. Catal.* 103(1), 153 (2011)
34. J. X. Yang, J. J. Ma, and Y. W. Huang, Hydrothermal synthesis of monodisperse leaf-like boehmite nanosheets: Transformation from irregular to regular morphology, Frontier of Nanoscience and Technology, Vol. 694, 28 (2011)
35. Y. M. Sun, H. Wang, P. Li, X. Z. Duan, J. Xu, and Y. F. Han, Synthesis and identification of hierarchical g-AlOOH self-assembled by nanosheets with adjustable exposed facets, *CrystEngComm* 18(24), 4546 (2016)
36. G. C. Li, L. L. Guan, Y. Q. Liu, and C. G. Liu, Template-free solvothermal synthesis of 3D hierarchical nanostructured boehmite assembled by nanosheets, *J. Phys. Chem. Solids* 73(9), 1055 (2012)
37. Y. X. Zhang, Y. J. Ye, X. B. Zhou, Z. L. Liu, G. P. Zhu, D. C. Li, and X. H. Li, Monodispersed hollow aluminosilica microsphere@hierarchical g-AlOOH deposited with or without $Fe(OH)_3$ nanoparticles for efficient adsorption of organic pollutants, *J. Mater. Chem. A* 4(3), 838 (2016)
38. R. W. Hicks and T. J. Pinnavaia, Nanoparticle assembly of mesoporous AlOOH (Boehmite), *Chem. Mater.* 15(1), 78 (2003)
39. Y. Cai, H. H. Huang, L. Wang, X. J. Zhang, Y. W. Yuan, R. Li, H. Wan, and G. F. Guan, Facile synthesis of pure phase g-AlOOH and g-Al_2O_3 nanofibers in a recoverable ionic liquid via a low temperature route, *RSC Adv.* 5(127), 104884 (2015)
40. X. Y. Chen, Z. H. Zhang, X. L. Li, and S. W. Lee, Controlled hydrothermal synthesis of colloidal boehmite (-AlOOH) nanorods and nanoflakes and their conversion into - Al_2O_3 nanocrystals, *Solid State Commun.* 145(7–8), 368 (2008)
41. S. Peng, X. J. Yang, D. Tian, and W. L. Deng, Chemically stable and mechanically durable superamphiphobic aluminum surface with a micro/nanoscale binary structure, *ACS Appl. Mater. Inter.* 6(17), 15188 (2014)
42. S. Yamazoe, M. Naya, M. Shiota, T. Morikawa, A. Kubo, T. Tani, T. Hishiki, T. Horiuchi, M. Suematsu, and M. Kajimura, Large-area surface-enhanced Raman spectroscopy imaging of brain ischemia by gold nanoparticles grown on random nanoarrays of transparent boehmite, *ACS Nano* 8(6), 5622 (2014)
43. Z. Xu, J. Yu, J. Low, and M. Jaroniec, Microemulsion-assisted synthesis of mesoporous aluminum oxyhydroxide nanoflakes for efficient removal of gaseous formaldehyde, *ACS Appl. Mater. Inter.* 6(3), 2111 (2014)
44. Z. J. Wang, Y. Tian, H. S. Fan, J. H. Gong, S. G. Yang, J. H. Ma, and J. Xu, Facile seed-assisted hydrothermal fabrication of g-AlOOH nanoflake films with superhydrophobicity, *New J. Chem.* 38(3), 1321 (2014)
45. Y. L. Feng, W. C. Lu, L. M. Zhang, X. H. Bao, B. H. Yue, Y. Iv, and X. F. Shang, One-step synthesis of hierarchical cantaloupe-like AlOOH superstructures via a hydrothermal route, *Cryst. Growth Des.* 8(4), 1426 (2008)
46. A. Alemi, Z. Hosseinpour, M. Dolatyari, and A. Bakhtiari, Boehmite (g-AlOOH) nanoparticles: Hydrothermal synthesis, characterization, pH-controlled morphologies, optical properties, and DFT calculations, *Phys. Status Solidi B* 249(6), 1264 (2012)